# Lattice models and Landau theory for type-II incommensurate crystals

G. H. F. van Raaij,* K. J. H. van Bemmel,† and T. Janssen
*Institute for Theoretical Physics, University of Nijmegen, Toernooiveld 1, NL-6525 ED Nijmegen, The Netherlands*
(Received 7 September 1999)

Ground-state properties and phonon dispersion curves of a classical linear-chain model describing a crystal with an incommensurate phase are studied. This model is the DIFFOUR (discrete frustrated $\phi^4$) model with an extra fourth-order term added to it. The incommensurability in these models may arise if there is frustration between nearest-neighbor and next-nearest-neighbor interactions. We discuss the effect of the additional term on the phonon branches and phase diagram of the DIFFOUR model. We find some features not present in the DIFFOUR model such as the renormalization of the nearest-neighbor coupling. Furthermore, the ratio between the slopes of the soft phonon mode in the ferroelectric and paraelectric phase can take on values different from $-2$. Temperature dependences of the parameters in the model are different above and below the paraelectric transition, in contrast with the assumptions made in Landau theory. In the continuum limit this model reduces to the Landau free-energy expansion for type-II incommensurate crystals and it can be seen as the lowest-order generalization of the simplest Lifshitz-point model. Part of the numerical calculations have been done by an adaption of the effective potential method, originally used for models with nearest-neighbor interaction, to models with also next-nearest-neighbor interactions.

## I. INTRODUCTION

Like other transitions, the phase transition to an incommensurate (INC) phase (reviews are given by Bak,[1] Selke,[2] and Janssen and Janner[3]) can be described on the phenomenological level within the frame of extended Landau theory.[4] The necessary extension consists essentially in accounting for the expansion of the free-energy density as a function not only of the components of the order parameter, but also of their spatial derivatives. Therefore the global free energy becomes a functional of spatially dependent components of the order parameter and the equilibrium configuration for given values of temperature and external parameters is found as a solution of a variational problem.

The continuum Landau theory allows a natural classification[5] of the possible forms of the free-energy functional for an INC transition into two classes, according to whether the driving term in the free-energy expansion responsible for the appearance of the incommensurate state is linear (type I, Lifshitz invariant present) or quadratic (type II, no Lifshitz invariant) in the gradient of the order parameter. The properties of those two kinds of INC phases are different: for type-I INC phases the lock-in transition is either continuous, or only slightly discontinuous, and approaching the lock-in temperature $T_c$ these phases exhibit the structuration of the modulated phase into discommensurations or solitons. On the other hand, the modulation of the type-II INC phase remains practically sinusoidal down to the temperature $T_c$ and the lock-in transition is always of first order. Although the above statements can be considered as a rule of thumb, there are cases known where there is coexistence of solitonic and sinusoidal structural modulation. See Aramburu[6] for details.

In the following we will only be concerned with models describing type-II INC phases. Landau theory has been rather successful in describing basic properties of these phases, but if one wants to have a better understanding of the true microscopic origin of the INC phase one has to go beyond this phenomenological approach. One possibility would be to study full microscopic models with realistic interactions. Another approach, to which the main part of this paper will be devoted, is to study semimicroscopic models which take into account the discrete nature of the systems and discuss properties in terms of (effective) interatomic interactions.

The discreteness of a lattice leads to a number of important physical consequences such as pinning of solitons in the anisotropic next-nearest-neighbor Ising (ANNNI) model (see Yeomans[7] for a review) and in the Frenkel-Kontorova model,[8] and the existence of a devil's staircase (infinite number of commensurate and incommensurate phases), for example found in betaine calcium chloride dihydrate (BCCD).[9] Within Landau theory it is difficult to explain the occurrence of a specific sequence of transitions: several lock-in terms are needed then. For example, Ribeiro *et al.*[10] chose the magnitude of four distinct lock-in contributions to the free energy in such a way as to stabilize the four most prominent commensurate phases in BCCD. Furthermore, in discrete models chaotic states are possible,[1,11] which may provide an alternative description of phenomena observed in for example spin glasses, superionic conductors, the magnetic system CeSb and systems with pinning of charge-density waves. See Bak[1] for details.

In the past few years different lattice models have been constructed to describe the phase transitions in, for example, the $A_2BX_4$ family,[12] in BCCD,[13] and, more general, in crystals with $Pcmn$ symmetry.[14] These models are two dimensional, with only nearest-neighbor interactions. Hlinka *et al.*[15] studied a three-dimensional nearest-neighbor model, applicable to BCCD. All these models have in common that the frustrated interaction, needed for having an incommensurate phase, comes from a nearest-neighbor mixing interaction.

Recent x-ray,[16] neutron,[17,18] and Raman[19] experiments on

 ©2000 The American Physical Society

the $Sn_2P_2(S_{1-x}Se_x)_6$ crystal family of uniaxial ferroelectrics motivated us to study lattice models. In the composition-temperature phase diagram of this crystal family a Lifshitz point is present.[20] At this point the paraelectric phase, the ferroelectric phase and the INC phase become equal, and the boundaries separating these phases have equal derivative. Such a special point was, except for some ferroelectric liquid crystals, only found in the temperature-applied magnetic field phase diagram of the magnetic compound MnP.[21] From both experimental and theoretical point of view this uniaxial Lifshitz point is interesting because critical exponents deviate[22] from those found for ordinary critical points. This crystal family furthermore displays an interesting modulation wave-vector behavior, shows crossover effects from order-disorder to a displacive type of phase transition,[23] and the ratio between the slopes of the soft phonon mode in the ferroelectric and paraelectric phase deviates[17] substantially from the standard value $R=-2$. These features are much easier to understand in a lattice model than in Landau theory.

The paper is arranged as follows: in Sec. II we present a one-dimensional model; in many anisotropic systems, like $Sn_2P_2(S_{1-x}Se_x)_6$, the modulation wave vector is in one specific direction. The incommensurability may arise if there is frustrating interaction between nearest-neighbor and next-nearest-neighbor couplings. We discuss general features of the model. In Sec. III we give some exact results regarding ground-state properties. In Sec. IV we discuss the dynamics and the stability of the various phases. In Sec. V the phase diagrams, calculated partly analytically, partly numerically, are presented. Temperature effects are treated in Sec. VI. In Sec. VII we discuss the continuum limit of the model which gives the connection with the Landau theory. We conclude and give an outlook for further research in Sec. VIII. In Appendix A we give some exact results for phase boundaries and in Appendix B we present the next-nearest-neighbor extension of the effective potential method for the determination of the ground state. This method was used to calculate some of the phase diagrams.

## II. AN EXTENSION OF THE DIFFOUR MODEL

In the following we will be concerned with an extension of the so-called DIFFOUR model[24] (discrete frustrated $\phi^4$ model), for which the potential energy can be written as

$$V=\sum_n \left\{\frac{A}{2}x_n^2+\frac{B}{4}x_n^4+\frac{C}{2}(x_n-x_{n-1})^2+\frac{D}{2}(x_n-x_{n-2})^2 + \frac{E}{2}[x_n^2(x_n-x_{n-1})^2+x_n^2(x_n-x_{n+1})^2]\right\}. \quad (2.1)$$

The original DIFFOUR model, or EHM (elastically hinged molecule) model,[25] has $E=0$. Although in principle this model gives incommensurate ground states, the behavior of the modulation wave vector as found in experiments cannot be reproduced satisfactorily by the model. In order to account for this shortcoming we supply the DIFFOUR model with a nonlinear coupling to neighbors. There are several possibilities: if we restrict ourselves to fourth-order terms we can consider a term $\propto(x_n-x_{n-1})^4$. The resulting model has been studied by Lamb,[26] who showed that the origin of this term is related to strain terms in the so-called magnetoelastic DIFFOUR model. Another possibility would be to consider a term of the form $\propto(x_n-x_{n-2})^4$. Without the term mentioned above this would, however, be rather unphysical. Instead we will choose a term of the form $\propto x_n^2(x_n-x_{n\pm1})^2$. This is the lowest-order dispersive fourth-order term, as will be shown in Sec. VII, and can, for example, be obtained from strain terms.

The order parameter $x_n$ can be, for example, a displacement, a component of the polarization $P$ for ferroelectric systems, a component of the magnetization $M$ for magnetic systems, a rotation angle or a strain component. In this article we use for convenience terms like paraelectric, ferroelectric, and antiferroelectric to distinguish between different ground states. The origin of incommensurability in this model is essentially competition between interactions with nearest- and next-nearest neighbors which may lead to frustration. Higher-order terms are needed for stabilization.

We expect that the extra fourth-order term ($E\neq0$) has a large effect on the phase diagrams for $E=0$. To actually determine phase diagrams it is not necessary to vary all five parameters $A,B,C,D,E$, which can be seen as follows: by taking $x_n'=\sqrt{B/|D|}x_n$ and $V'=B/|D|^2V$ we get the following renormalized parameters: $A'=A/|D|$, $B'=1$, $C'=C/|D|$, $D'=D/|D|=\pm1$, and $E'=E/B$.

For some purposes it is convenient to rewrite the potential in the following form:

$$V=\sum_n \left\{\frac{\tilde A}{2}x_n^2+\frac{\tilde B}{4}x_n^4+\tilde C x_n x_{n-1}+\tilde D x_n x_{n-2} + \frac{\tilde E}{2}[x_n^2(x_n-x_{n-1})^2+x_n^2(x_n-x_{n+1})^2]\right\}, \quad (2.2)$$

with $\tilde A=A+2C+2D$, $\tilde B=B$, $\tilde C=-C$, $\tilde D=-D$, and $\tilde E=E$. From this the connection with the ANNNI model can easily be made. Let us put $\tilde E=0$ and $\tilde B=-\tilde A$. If we now take the limit $\tilde A\to-\infty$ we end up with a model with two infinitely deep wells. The $x_n$ can only take on values $\pm1$ and can thus be seen as spins. These spins are coupled to nearest neighbors and next-nearest neighbors via the $\tilde C$ and $\tilde D$ terms. So by increasing the depth of the double-well potential there is a crossover from displacive behavior to order-disorder behavior in the transition from the normal to the incommensurate phase.

Inserting $x_n'=(-1)^n x_n$ in the above potential leads to

$$V=\sum_n \left\{\frac{\tilde A}{2}x_n'^2+\frac{\tilde B}{4}x_n'^4-\tilde C x_n' x_{n-1}'+\tilde D x_n' x_{n-2}' + \frac{\tilde E}{2}[x_n'^2(x_n'+x_{n-1}')^2+x_n'^2(x_n'+x_{n+1}')^2]\right\}. \quad (2.3)$$

In the DIFFOUR model ($\tilde E=0$) this leads to the following symmetry: if $\{x_n\}$ is a state for $\tilde C=X$, then $\{(-1)^n x_n\}$ is a state for $\tilde C=-X$ with the same energy. This property can for example be seen in the ferroelectric-antiferroelectric phases. However, for $\tilde E\neq0$ this symmetry $\tilde C\leftrightarrow-\tilde C$ is no longer present.

### III. GROUND-STATE PROPERTIES

Different ground states are possible, depending on the values of the parameters. The stationary states are solutions of $\partial V/\partial x_n = 0$, giving

$$Ax_n + Bx_n^3 + C(2x_n - x_{n-1} - x_{n+1}) + D(2x_n - x_{n-2} - x_{n+2}) + E[4x_n^3 - 3x_n^2(x_{n-1} + x_{n+1}) + 2x_n(x_{n-1}^2 + x_{n+1}^2) - (x_{n-1}^3 + x_{n+1}^3)] = 0. \quad (3.1)$$

If we impose periodic boundary conditions $x_{N+n} = x_n$ we arrive at a set of $N$ coupled nonlinear equations. To find the lowest-energy state for each solution and for each value of $N$ the potential energy has to be evaluated. For low-period commensurate states (small values of $N$) analytic solutions of the above equation can be found. In the following, we study (for fixed $N$) periodic solutions of Eq. (3.1). For them we give the equilibrium values $\{x_n\}$ and the corresponding energy per particle $v = V/N$.

In the paraelectric state ($N=1$) all particles are in the equilibrium positions

$$x_n = 0, \quad v = 0. \quad (3.2)$$

In the ferroelectric state ($N=1$) all particles are uniformly displaced from their equilibrium positions

$$x_n = \sqrt{-\frac{A}{B}}, \quad v = -\frac{A^2}{4B}. \quad (3.3)$$

Note that $B$ always has to be positive, for the potential to be bounded from below. This implies that the ferroelectric state only can exist for $A<0$. For $A>0$ the ground state may be paraelectric. In the following we give some analytic results, based on numerical calculations of the shape of the solution $\{x_n\}$.

In the antiferroelectric state ($N=2$) particle positions alternate along the chain

$$x_n = (-1)^n \sqrt{-\frac{A+4C}{B+16E}}, \quad v = -\frac{(A+4C)^2}{4(B+16E)}. \quad (3.4)$$

The potential is unbounded from below for $E \leqslant -B/16$ and stable solutions exist only for $E > -B/16$ and $A+4C<0$. Both conditions have to be satisfied.

For $N=3$ we determined the solution with lowest energy to be of the form $(x_1,x_2,x_3) = (k\xi,\xi,k\xi)$, with $x_1/x_2<0$, and

$$\xi^2 = -\frac{A+2(C+D)(1-k)}{B+2E(2-3k+2k^2-k^3)} = -\frac{Ak+(C+D)(k-1)}{Bk^3+E(2k^3-3k^2+2k-1)}. \quad (3.5)$$

The factor $k$ is determined by

$$2[B(C+D)+E(-A+C+D)]k^4 - [B(A+2C+2D) + 2E(-A+2C+2D)]k^3 - 3AEk^2 + [B(A+C+D) + 2E(A+2C+2D)]k - [B(C+D)+E(-A+2C+2D)] = 0. \quad (3.6)$$

The energy per particle is given in terms of $\xi$ and $k$ as

$$v = \frac{\xi^2}{6}[A(1+2k^2) + 2(C+D)(1-k)^2] + \frac{\xi^4}{12}[B(1+2k^4) + 4E(1+k^2)(1-k)^2]. \quad (3.7)$$

Note that the quartic Eq. (3.6) can be written as

$$(1-k)\{-2[B(C+D)+E(-A+C+D)]k^3 + [BA+2E(C+D)]k^2 + [BA+E(3A+2C+2D)]k - [B(C+D)+E(-A+2C+2D)]\} = 0, \quad (3.8)$$

where the special solution $k=1$ gives a ferroelectric state. The solution of the remaining cubic equation, which can be solved exactly for given parameters, gives a $k$ such that $x_1/x_2<0$, a true $N=3$ state.

The lowest energy state for $N=4$ has $x_1 = x_2 = \rho$, $x_3 = x_4 = -\rho$ with

$$\rho = \sqrt{-\frac{A+2C+4D}{B+8E}}, \quad v = -\frac{(A+2C+4D)^2}{4(B+8E)}. \quad (3.9)$$

We have to keep in mind that we must satisfy $E > -B/16$, which is not obvious from the above expression, but comes from the analysis of the antiferroelectric state.

The lowest energy solution for $N=6$ can analytically be obtained, in the same manner as for $N=3$. It has the form $(x_1,x_2,x_3,x_4,x_5,x_6) = (k\xi,\xi,k\xi,-k\xi,-\xi,-k\xi)$. The lowest energy solution for $N=8$ reads $(x_1,x_2,x_3,x_4,x_5,x_6,x_7,x_8) = (k\xi,\xi,\xi,k\xi,-k\xi,-\xi,-\xi,-k\xi)$. For $N=5$ one needs two different values of $k$: $(x_1,x_2,x_3,x_4,x_5) = (k\xi,k'\xi,\xi,k'\xi,k\xi)$ and for $N=7$ one needs three different values: $k,k',k''$, and the above method no longer works for $N=5$ and $N=7$. Therefore, to find states with larger periods, or even incommensurate periods, we rely on numerical calculations, for which true incommensurate states of course never can be found. However, the idea is that such a state can always be arbitrarily well approximated by a commensurate state with wavelength

$$\lambda = \frac{N}{s}, \quad s = 1,2,\ldots, \quad N \geqslant 2s, \quad (3.10)$$

where $N,s$ are coprime numbers. Such a solution has a period $N$ and, in general, $2s =$ (number of local minima + number of local maxima). In the special case where the $\{x_n\}$ take on positive and negative values, $2s =$ (number of sign changes within the period $N$). The bigger $N$ and $s$, the better the approximation.

As an example of a numerical calculation we consider the ground state for $A = 2.249\,99$, $B=1$, $C=1$, $D=-1$, $E=1$. It is known to be incommensurate (see Secs. IV and V) with a wavelength $\arccos(\frac{1}{4}) \approx 4.766\,792\,13$. By the Farey construction[3] we find that $\frac{62}{13} \approx 4.769\,230\,77$ should be a reasonable commensurate approximation. We numerically

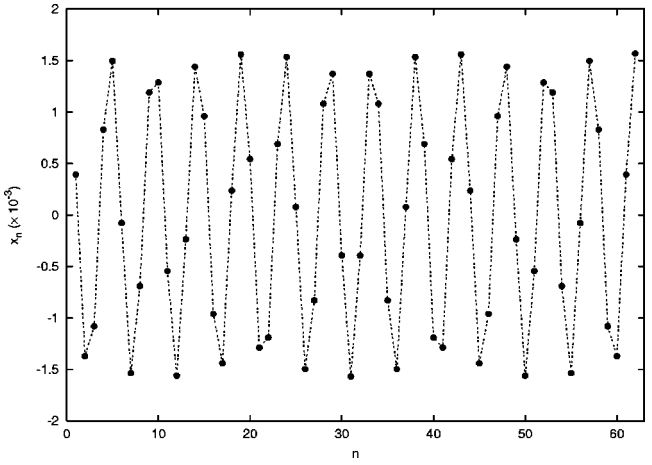


FIG. 1. Ground-state configuration for $A=2.249\,99$, $B=1$, $C=1$, $D=-1$, and $E=1$ in the commensurate approximation 62/13. $x_n$ is the displacement for particle $n$. For $A,B,C,D,E$ given above the system is just below the phase boundary between the paraelectric phase and the incommensurate phase. Although the displacements are small, $\mathcal{O}(10^{-3})$, the onset of the incommensurate phase is evident. Points are calculations, lines are drawn to guide the eye.

determined the ground state in terms of the $\{x_n\}$. The result is shown in Fig. 1. After 62 particles the sequence repeats itself, and the solution passes through zero 26 times. We can label this state by its modulation wave vector $\frac{13}{62}$, measured in units of $2\pi$.

For certain regimes in the parameter space the ground state can be determined analytically. The entire phase boundary of the paraelectric state and a part of the phase boundary of the ferroelectric state can be calculated. For the nearest-neighbor case in the DIFFOUR model proofs are given by Janssen and Tjon.[27] We extend their proofs to the case in which we also have next-nearest-neighbor interaction. As the proof is rather lengthy it will be given in Appendix A.

## IV. PHONON DISPERSION CURVES AND STABILITY LIMITS

To decide whether a solution of the equilibrium conditions is locally stable or not, one considers small displacements $\epsilon_n$ from the positions given by a static solution $\{x_n\}$ satisfying Eq. (3.1):

$$u_n = x_n + \epsilon_n . \tag{4.1}$$

The phonon frequencies are given by the square roots of the eigenvalues of the dynamical matrix and for stability all eigenvalues have to be non-negative. The dynamical matrix for a period-$N$ solution ($N \geqslant 5$) has elements

$$\begin{aligned} D_{n,n} &= A + 3Bx_n^2 + 2C + 2D + 2E[6x_n^2 - 3x_n(x_{n-1}+x_{n+1}) \\ &\quad + x_{n-1}^2 + x_{n+1}^2], \\ D_{n,n\pm1} &= -C + E[-3x_n^2 + 4x_n x_{n\pm1} - 3x_{n\pm1}^2], \\ D_{n,n\pm2} &= -D, \end{aligned} \tag{4.2}$$

with $x_{N+n}=x_n$ and the special cases

TABLE I. Stability limits for the paraelectric phase (4.5). Note that $B+16E>0$ must be satisfied.

| Parameter range | $q$ value of instability | Conditions for having a stable state |
|---|---|---|
| $D<0$: | | |
| $C<4D$ | $q_c=\pi$ | $A>-4C$ |
| $4D \leqslant C \leqslant -4D$ | $\cos(q_c)=\dfrac{-C}{4D}$ | $A+\dfrac{(4C+16D)^2}{64D}>0$ |
| $C>-4D$ | $q_c=0$ | $A>0$ |
| $D>0$: | | |
| $C<0$ | $q_c=\pi$ | $A>-4C$ |
| $C>0$ | $q_c=0$ | $A>0$ |

$$\begin{aligned} D_{1,N} &= [-C + E(-3x_1^2 + 4x_1x_N - 3x_N^2)]e^{-iq}, \\ D_{1,N-1} &= D_{2,N} = -De^{-iq}. \end{aligned} \tag{4.3}$$

In the above expressions the $\{x_n\}$ are solutions of Eq. (3.1). Furthermore, $D_{n,m}=D_{m,n}^*$ and all other matrix elements are zero. In the following the phonon branches for certain low-period states will be examined. This will be done in terms of $A,B,C,D,E$.

### A. Paraelectric state

For the paraelectric state (3.2) the dynamical matrix is given by

$$\mathsf{D} = A + 2C[1-\cos(q)] + 2D[1-\cos(2q)] = m\omega^2. \tag{4.4}$$

Rewriting this equation gives

$$m\omega^2 = A + (4C+16D)\sin^2\left(\frac{q}{2}\right) - 16D\sin^4\left(\frac{q}{2}\right). \tag{4.5}$$

Note that this expression does not contain $E$. This means that the stability limits for the paraelectric phase in this model are the same as those for the paraelectric state in the DIFFOUR model. Now, we are looking for the minimum of this phonon branch. We distinguish the cases $D>0$ and $D<0$. The results are summarized in Table I.

For $D>0$ and $C=0$, the branch has two minima, at $\sin^2(q/2)=0$ and $\sin^2(q/2)=1$. For $A<0$ the ferroelectric state and the antiferroelectric state are degenerate, for $E=0$ only. Comparison with calculations in Appendix A shows that as long as the paraelectric state is stable, it is the ground state. Destabilization is the condensation of a soft phonon.

### B. Ferroelectric state

For the ferroelectric state (3.3) one has

TABLE II. Stability limits for the ferroelectric phase (4.6). Note that $B+16E>0$ and $A<0$ must be satisfied.

| Parameter range | $q$ value of instability | Conditions for having a stable state |
|---|---|---|
| $D<0$: | | |
| $C<\frac{2AE}{B}+4D$ | $q_c=\pi$ | $A<2C-\frac{4AE}{B}$ |
| $\frac{2AE}{B}+4D\leqslant C\leqslant\frac{2AE}{B}-4D$ | $\cos(q_c)=\frac{-C}{4D}+\frac{AE}{2BD}$ | $-2A+\frac{(C+4D-2AE/B)^2}{4D}>0$ |
| $C>\frac{2AE}{B}-4D$ | $q_c=0$ | $A<0$ |
| $D>0$: | | |
| $C<\frac{2AE}{B}$ | $q_c=\pi$ | $A<2C-\frac{4AE}{B}$ |
| $C>\frac{2AE}{B}$ | $q_c=0$ | $A<0$ |

$$m\omega^2=A+3Bx^2+2C[1-\cos(q)]+2D[1-\cos(2q)]+4Ex^2[1-\cos(q)]=-2A+\left(4C+16D-\frac{8AE}{B}\right)\sin^2\left(\frac{q}{2}\right)-16D\sin^4\left(\frac{q}{2}\right). \quad (4.6)$$

See Table II for the analysis. Note that for $D>0$ there is degeneracy for $E=0$.

### C. Antiferroelectric state

Finally, the phonon branches of the antiferroelectric state (3.4) will be investigated. The $2\times2$ dynamical matrix is given by

$$D_{1,1}=D_{2,2}=A+2C+2D[1-\cos(q)]-(3B+28E)\frac{A+4C}{B+16E},$$

$$D_{1,2}=D_{2,1}^*=(e^{-iq}+1)\left(-C+10E\frac{A+4C}{B+16E}\right). \quad (4.7)$$

The eigenvalue equation reads

$$m\omega^2=A+2C+4D-(3B+28E)\frac{A+4C}{B+16E}-4D\cos^2\left(\frac{q}{2}\right)\pm2\left(-C+10E\frac{A+4C}{B+16E}\right)\cos\left(\frac{q}{2}\right). \quad (4.8)$$

Results are summarized in Table III. Note that for $C=10E[(A+4C)/(B+16E)]$ the two branches coincide.

### D. States with period $N\geqslant3$

For the $N=3$ solution exact phonon frequencies can in principle be found. The elements of the dynamical matrix are given in terms of $\xi$ and $k$, defined in Eqs. (3.5) and (3.6):

$$D_{1,1}=D_{3,3}=A+2(C+D)+[3Bk^2+2E(4k^2-3k+1)]\xi^2,$$

$$D_{2,2}=A+2(C+D)+[3B+4E(k^2-3k+3)]\xi^2,$$

$$D_{1,2}=D_{2,3}=-C-E(3k^2-4k+3)\xi^2-De^{-iq}, \quad (4.9)$$

$$D_{1,3}=-D-(C+2Ek^2\xi^2)e^{-iq}.$$

The eigenvalues are then found as the solution (Cardano's formula) of a cubic equation.

For $N=4$ the dynamical matrix has elements in terms of $\rho$, defined in Eq. (3.9):

$$D_{n,n}=A+2(C+D)+(3B+16E)\rho^2,$$

$$D_{1,2}=D_{3,4}=-C-2E\rho^2,$$

$$D_{1,3}=D_{2,4}=-D(1+e^{-iq}), \quad (4.10)$$

$$D_{1,4}=(-C-10E\rho^2)e^{-iq},$$

$$D_{2,3}=-C-10E\rho^2.$$

The resulting secular equation is a quartic one and exact solutions for the eigenvalues can be found using Ferrari's formula.

For solutions with larger periods we have to rely on numerical calculations. As an example we again consider the ground state for $A=2.249\,99$, $B=1$, $C=1$, $D=-1$, $E=1$. See also the end of Sec. III. The calculated phonon dispersion curves in the commensurate approximation $\lambda=\frac{62}{13}$ are given in Fig. 2.

## V. CALCULATION OF PHASE DIAGRAMS

In this section we present some phase diagrams, calculated partly analytically, partly numerically. The traditional method to find the ground state numerically is to solve the equations for equilibrium (3.1). However, these equations also hold for metastable states, maxima, and saddle points and it may happen that one finds a metastable state instead of the true ground state. This problem is not present for the so-called effective potential method (EPM), introduced by Griffiths and Chou.[28] This method, in principle, always gives the ground state. Originally it was used to study Frenkel-

TABLE III. Stability limits for the antiferroelectric phase (4.8). Both $B+16E>0$ and $A+4C<0$ must be satisfied.

| Parameter range | $q$ value of instability | Conditions for having a stable state |
|---|---|---|
| $D<0$: | | |
| $C-10E\dfrac{A+4C}{B+16E}<4D$ | $q_c=0$ | $A<-4C$ |
| $4D\leqslant C-10E\dfrac{A+4C}{B+16E}\leqslant 0$ | $\cos\left(\dfrac{q_c}{2}\right)=\dfrac{C}{4D}-10E\dfrac{A+4C}{4D(B+16E)}$ | $A>-2C-4D+(3B+28E)\dfrac{A+4C}{B+16E}$ $-\dfrac{1}{4D}\left(-C+10E\dfrac{A+4C}{B+16E}\right)^2$ |
| $0\leqslant C-10E\dfrac{A+4C}{B+16E}\leqslant -4D$ | $\cos\left(\dfrac{q_c}{2}\right)=\dfrac{-C}{4D}+10E\dfrac{A+4C}{4D(B+16E)}$ | $A>-2C-4D+(3B+28E)\dfrac{A+4C}{B+16E}$ $-\dfrac{1}{4D}\left(-C+10E\dfrac{A+4C}{B+16E}\right)^2$ |
| $C-10E\dfrac{A+4C}{B+16E}>4D$ | $q_c=0$ | $\dfrac{A}{A+4C}<\dfrac{3B+8E}{B+16E}$ |
| $D>0$: | | |
| $C<10E\dfrac{A+4C}{B+16E}$ | $q_c=0$ | $A<-4C$ |
| $C>10E\dfrac{A+4C}{B+16E}$ | $q_c=0$ | $\dfrac{A}{A+4C}<\dfrac{3B+8E}{B+16E}$ |

Kontorova and similar one-dimensional models with only nearest-neighbor interaction. As an interesting application of this method, we mention a study of the ground state of the chiral $XY$ model in a field.[29] Below we give a brief outline of the method.

Consider a one-dimensional system with only nearest-neighbor interaction in its ground state. If one atom is displaced from its equilibrium position (we assume that $x_n$ denotes the displacement), the surrounding atoms will change their positions in order to minimize the total energy. This deformation will in general cost some energy. A function, called the ''effective potential,'' describes the net energy cost as a function of the positions of the atoms. This effective potential achieves its minimum on points of the ground state[30] and rigorous mathematical statements can be made.[31] Numerical procedures to find solutions are based on discretization of the range $x_n$ of the atomic positions. The $x_n$ can now only adopt a finite number of values.[32–34] For models with interactions up to next-nearest neighbors, as in the case of the extended DIFFOUR model, the EPM can be adapted, which will be discussed in Appendix B. The proofs of the existence of solutions for models with next-nearest-neighbor interactions, both in the continuous and discretized version, are rather long and will be given in a separate paper.[35]

Using the EPM and Eq. (3.1) we calculated various phase diagrams. First we varied both $A$ and $E$ with the other parameters fixed: $B=1$, $C=1$, and $D=-1$. The resulting phase diagram is given in Fig. 3. From the analysis in Appendix A we know that the phase boundary for the paraelectric state for $|C|<4$ is given by $A=\frac{1}{4}C^2-2C+4$. For $C=1$ and $D=-1$ we find $A=2\frac{1}{4}$. At this boundary we have a transition to an incommensurate state with wave vector $q=\arccos(-C/4D)=\arccos(\frac{1}{4})\approx 4.766\,792\,13$. This is the state we discussed at the end of Sec. III. We can clearly see the effect of the $E$ term: for $E=0$ further decreasing of $A$ leads to a transition to a commensurate state with period 4. For $E<0$ this transition can be followed by transitions to $N=3$ or $N=2$ commensurate states. For $E$ sufficiently positive, the wavelength of the ground state increases for decreasing $A$. Between the commensurate states incommensurate ones can be found. By increasing $E$, the region between paraelectric and ferroelectric phases shrinks. A positive $E$ term favors long-wavelength solutions, with the ferroelectric state being the extreme limit ($q=0$).

Figure 4 gives the phase diagram found for $B=1$, $D=-1$, $E=0$ and varying both $A$ and $C$. This is the phase diagram for the original DIFFOUR model.[3] We have seen that the phase boundary for the paraelectric phase for $|C|<4$ is a parabola symmetric around $C=0$. For $|C|\geqslant 4$ this boundary is given by $A+2C-2=-2+2|C|$, two straight lines. The parabola and the lines meet at $|C|=4$, and have equal derivative at this point. Note the symmetry $C\leftrightarrow -C$, which implies[36] that the modulation wave vectors for the system with $+C$ and $-C$ are related by

$$q_C+q_{-C}=\frac{1}{2} \tag{5.1}$$

in units of $2\pi$. At $(C=4,A=0)$ the paraelectric phase, the ferroelectric phase and the incommensurate phase become

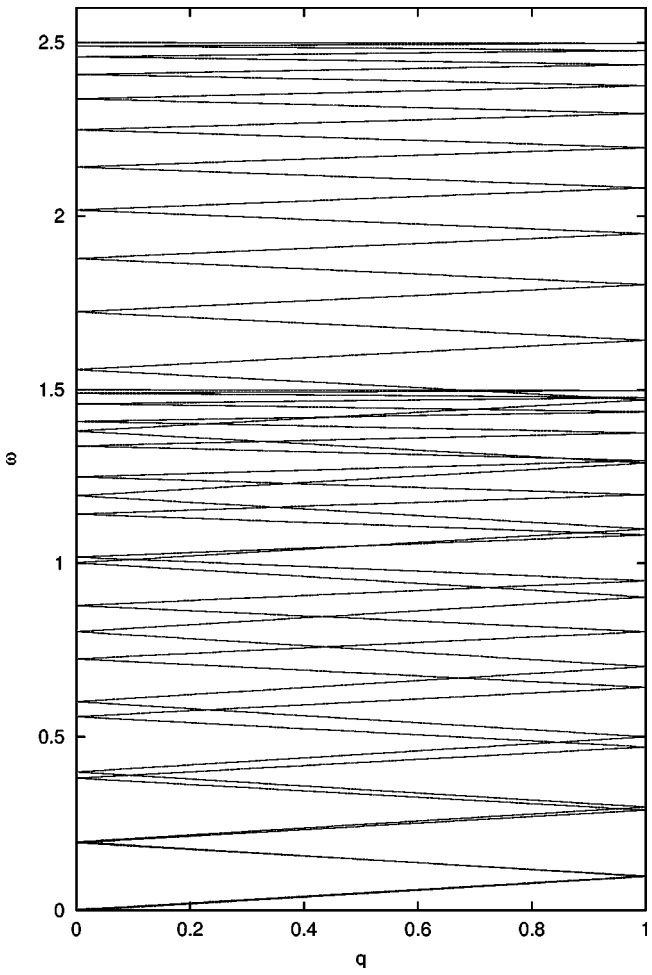


FIG. 2. Phonon dispersion curves for $A=2.249\,99$, $B=1$, $C=1$, $D=-1$, and $E=1$ in the commensurate approximation 62/13. This corresponds with the solution depicted in Fig. 1. $q$ is given in reduced units. There is one branch with $\omega\rightarrow 0$ for $q\rightarrow 0$: the phason branch. Just above this lies the amplitudon branch.

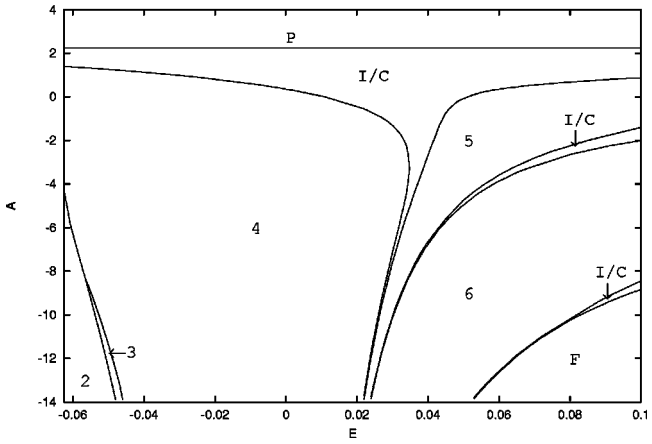


FIG. 3. The phase diagram for the extended DIFFOUR model with $B=1$, $C=1$, $D=-1$. Shown are the paraelectric phase (P), ferroelectric phase (F), antiferroelectric phase (2), and commensurate phases with period 3,4,5,6. Incommensurate phases are labeled I, higher-order commensurate phases C. There is no stable ground state for $E<-1/16$.

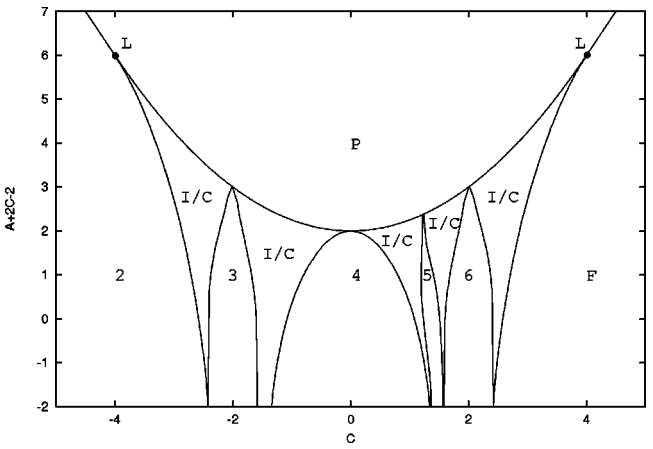


FIG. 4. The phase diagram for the extended DIFFOUR model with $B=1$, $D=-1$, and $E=0$. This is the original DIFFOUR model. Note the symmetry $C\leftrightarrow -C$. Same labeling as in Fig. 3. L denotes the Lifshitz points.

equal. The lines separating the paraelectric phase from the incommensurate phase and the incommensurate phase from the ferroelectric phase have equal derivative at this point. In Landau theory (see Sec. VII) such a point would be called a Lifshitz point. From the symmetry $C\leftrightarrow -C$ it is obvious that there is also a Lifshitz point at $(C=-4, A=16)$. At this point the paraelectric phase, the antiferroelectric phase and the incommensurate phase become equal.

Figure 5 gives the phase diagram for $B=1$, $D=-1$, $E=1$ in terms of $A$ and $C$. The symmetry $C\leftrightarrow -C$ is no longer present. However, the phase boundary of the paraelectric phase is independent of $E$. Also the wavelength of the phase emanating from this boundary is the same. In particular the positions of the Lifshitz points and the derivates at these points do not change. Note the boundary of the antiferroelectric phase: starting from the Lifshitz point and going down in the phase diagram, it initially bends to the right and then returns to lower values of $C$. Figs. 4 and 5 have been obtained by solving Eq. (3.1) and comparing the energies of the solutions.

We investigated the nearby surroundings of the Lifshitz point at $(C=4, A=0)$to look how the transition line from

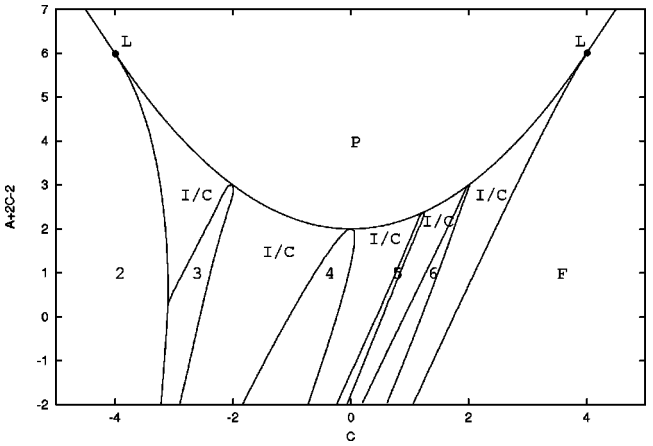


FIG. 5. The phase diagram for the extended DIFFOUR model with $B=1$, $D=-1$, and $E=1$. Note the asymmetric character, although the boundary of the paraelectric phase is the same as in Fig. 4. Same labeling as in Fig. 4.

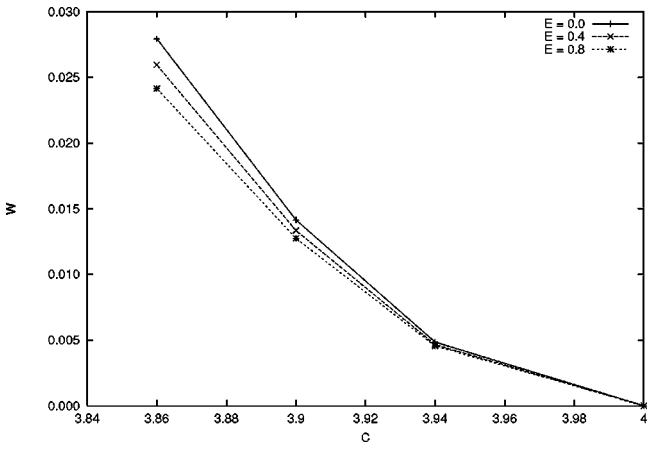


FIG. 6. Influence of the $E$ term on the wedge width $W$ near the Lifshitz point for $B=1$ and $D=-1$. Points are calculations, lines are drawn to guide the eye.

the ferroelectric phase to the incommensurate phase changes by increasing $E$. See Fig. 6 for the results. One notices a tendency towards a smaller wedge $W$ (the vertical distance between the paraelectric-incommensurate phase boundary and the incommensurate-ferroelectric phase boundary) by increasing $E$, as was to be expected.

### VI. TEMPERATURE-DEPENDENT BEHAVIOR

As the model under consideration is one dimensional with short-range interactions, there is no phase transition possible at $T\neq 0$. If we, however, consider weakly interacting linear chains in a three-dimensional system, this system can be described by Eq. (2.1) as well if we interpret the variables $x_n$ as averages over planes perpendicular to a fixed direction (the $c$ axis). Phase transitions become possible due to interchain couplings.

To study the temperature dependence of the parameters we take the thermal average of the conditions for equilibrium (3.1), resulting in

$$\begin{aligned} &A\langle x_n\rangle + B\langle x_n^3\rangle + C(2\langle x_n\rangle - \langle x_{n-1}\rangle - \langle x_{n+1}\rangle) + D(2\langle x_n\rangle \\ &\quad - \langle x_{n-2}\rangle - \langle x_{n+2}\rangle) + E[4\langle x_n^3\rangle - 3\langle x_n^2 x_{n-1}\rangle \\ &\quad - 3\langle x_n^2 x_{n+1}\rangle + 2\langle x_n x_{n-1}^2\rangle + 2\langle x_n x_{n+1}^2\rangle - \langle x_{n-1}^3\rangle \\ &\quad - \langle x_{n+1}^3\rangle] = 0. \end{aligned} \tag{6.1}$$

We have to distinguish between ground states with $\{\overline{x_n}\}=0$ and ground states with $\{\overline{x_n}\}\neq 0$, where the $\{\overline{x_n}\}$ are solutions of Eq. (3.1).

In the former case we assume that the thermal fluctuations of the displacement $x_n$ do not depend on the lattice site, $\langle x_n^2\rangle - \langle x_n\rangle^2 \approx \langle x_m^2\rangle - \langle x_m\rangle^2$, and if we furthermore approximate the correlations by $\langle x_n^2 x_m\rangle \approx \langle x_n^2\rangle\langle x_m\rangle$, the following holds:

$$\begin{aligned} &E[-3\langle x_n^2 x_{n-1}\rangle - 3\langle x_n^2 x_{n+1}\rangle + 2\langle x_n x_{n-1}^2\rangle + 2\langle x_n x_{n+1}^2\rangle \\ &\quad - \langle x_{n-1}^3\rangle - \langle x_{n+1}^3\rangle] + (B+4E)\langle x_n^3\rangle \\ &\approx E[-3\langle x_n\rangle^2(\langle x_{n-1}\rangle + \langle x_{n+1}\rangle) + 2\langle x_n\rangle(\langle x_{n-1}\rangle^2 \\ &\quad + \langle x_{n+1}\rangle^2) - (\langle x_{n-1}\rangle^3 + \langle x_{n+1}\rangle^3)] + 4E(\langle x_n^2\rangle \\ &\quad - \langle x_n\rangle^2)(2\langle x_n\rangle - \langle x_{n-1}\rangle - \langle x_{n+1}\rangle) + (B+4E)\langle x_n\rangle^3 \\ &\quad + B(\langle x_n^2\rangle - \langle x_n\rangle^2)\langle x_n\rangle. \end{aligned} \tag{6.2}$$

Inserting the last expression in Eq. (6.1) we see that the conditions for equilibrium for the thermal average of the displacement, $\langle x_n\rangle$, have the same form as those for the displacements $x_n$ themselves; the only difference being the replacement of the parameters $A$ and $C$ by temperature dependent ones:

$$\begin{aligned} A &\rightarrow A + BT, \\ C &\rightarrow C + 4ET, \end{aligned} \tag{6.3}$$

where $T=\langle x_n^2\rangle - \langle x_n\rangle^2$ is a measure of the thermal fluctuations. So a change in temperature will renormalize both parameters $A$ and $C$ (unlike in the DIFFOUR model with $E=0$).

For all other ground-state solutions ($\overline{x_n}\neq 0$) we calculate the thermal averages around $\overline{x_n}$, where the $\{\overline{x_n}\}$ satisfy Eq. (3.1),

$$\begin{aligned} \langle x_n^p x_m^q\rangle &= \frac{\int\int x_n^p x_m^q e^{-\beta(x_n-\overline{x_n})^2/2} e^{-\beta(x_m-\overline{x_m})^2/2} dx_n dx_m}{\int\int e^{-\beta(x_n-\overline{x_n})^2/2} e^{-\beta(x_m-\overline{x_m})^2/2} dx_n dx_m} \\ &= \langle x_n^p\rangle\langle x_m^q\rangle, \end{aligned} \tag{6.4}$$

where $\beta=1/T$. Three different integrals have to be calculated, yielding

$$\begin{aligned} \langle x_n^3\rangle &= \overline{x_n^3} + 3\overline{x_n}T, \\ \langle x_n^2\rangle &= \overline{x_n^2} + T, \\ \langle x_n\rangle &= \overline{x_n}. \end{aligned} \tag{6.5}$$

Substitution in Eq. (6.1) and comparison with Eq. (3.1) then leads to

$$\begin{aligned} A &\rightarrow A + (3B+4E)T, \\ C &\rightarrow C + 6ET. \end{aligned} \tag{6.6}$$

Note that the parameter $E$ now also enters in the temperature dependence of $A$. This linear behavior in $T$, with a kink at the temperature where the transition from the paraelectric phase to the incommensurate or the ferroelectric phase takes place, is corroborated by Monte Carlo calculations.[37,38] Some of the results[38] are shown in Fig. 7. The results (6.3) and (6.6) are in sharp contrast with the assumptions made in standard Landau theory, to be discussed in Sec. VII, that there is only one temperature-dependent parameter, and that its behavior above and below the transition temperature is the same.

It is now straightforward to calculate the temperature-dependent ground states and stability limits by making substitutions (6.3) and (6.6). We especially would like to focus on the phonon branches in the paraelectric and ferroelectric phases. Of experimental interest is the ratio between the

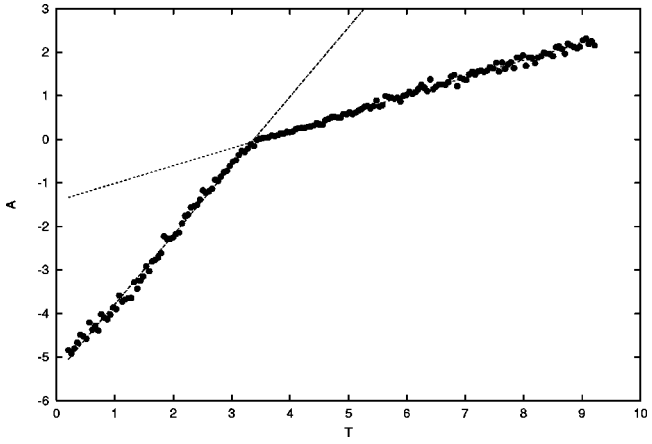


FIG. 7. Temperature dependence $A(T)$ calculated on a three-dimensional version of Eq. (2.1) with harmonic nearest-neighbor coupling and $A(0)=-5$, $B=5$, $D=E=0$. Points are calculations, (Ref. 38) lines are fits with a linear function. The phase transition takes place at $A=0$.

slopes of the soft phonon mode in the ferroelectric and paraelectric phase, the so-called $R$ parameter:

$$R=\frac{d\omega^2/dT|_{\text{ferro}}}{d\omega^2/dT|_{\text{para}}}. \tag{6.7}$$

Self-consistent renormalized phonon theory[39] gives the result $R=-2$. In experiments,[17] however, very often $R\neq -2$ is found. Taking into account the temperature dependence given in Eqs. (6.3) and (6.6), we find using Eqs. (4.5) and (4.6)

$$R=\frac{-2(3B+4E)-32E^2/B\sin^2(q/2)}{B+16E\sin^2(q/2)}, \tag{6.8}$$

which, for $E=0$, gives (at the center of the Brillouin zone) $R=-6$ instead of $R=-2$, and for $E\neq 0$ can take on any value as long as $B+16E>0$ is satisfied. Molecular-dynamics simulations on a three-dimensional $\phi^4$ lattice by Padlewski *et al.*[40] show that $R=-2$ holds only for systems with long-range couplings being in the displacive limit. However, Sollich *et al.*[41] showed that this double limit of displaciveness and long-range interaction is not necessary if the system is displacive enough: they found $R=-2$ for a system with only nearest-neighbor interactions, thereby questioning Padlewski's claim[40] of having studied a system in the displacive limit.

## VII. COMPARISON WITH THE CONTINUUM THEORY

The continuum limit of the extended DIFFOUR model leads to a well-known expansion. By replacing the differences in the general order parameter $x_n$ by differentials in the principal order parameter for ferroelectrics, the polarization $P(z)$,

$$(x_n-x_{n-1})^2\rightarrow\left(\frac{dP}{dz}\right)^2,$$

$$(x_{n-1}+x_{n+1}-2x_n)^2\rightarrow\left(\frac{d^2P}{dz^2}\right)^2, \tag{7.1}$$

and rearranging terms we arrive at the free-energy density

$$f=\frac{\alpha}{2}P^2+\frac{\beta}{4}P^4+\frac{\kappa}{2}\left(\frac{dP}{dz}\right)^2+\frac{\lambda}{2}\left(\frac{d^2P}{dz^2}\right)^2+\frac{\eta}{2}P^2\left(\frac{dP}{dz}\right)^2, \tag{7.2}$$

with $\alpha=A$, $\beta=B$, $\kappa=C+4D$, $\lambda=-D$, and $\eta=2E$. The above free-energy density was used by Ishibashi and Shiba[42] to study phase transitions in $NaNO_2$ and $SC(NH_2)_2$ (thiourea), proper ferroelectrics in which the polarization component of interest transforms according to a one-dimensional irreducible representation. The $\eta$ term is allowed by symmetry because it is the product of the two invariants $P^2$ and $(d^2P/dz^2)^2$. Alternatively, as both sodium nitrite and thiourea admit an interaction of $P$ with another mode $u$ (strain for example), Dvořák[43] showed that the $\eta$ term accounts in an effective manner for this interaction, thereby reducing $g(P,u)\rightarrow f(P)$.

By taking the Fourier transform of the above free-energy density we find

$$\tilde{f}=\left(\frac{\alpha}{2}+\frac{\kappa}{2}q^2+\frac{\lambda}{2}q^4\right)P_q^2+\left(\frac{\beta}{4}+\frac{\eta}{2}q^2\right)P_q^4. \tag{7.3}$$

This justifies the choice of the $E$ term in the extended version of the DIFFOUR model, discussed in Sec. II. A term $\propto(dP/dz)^4$ has been included in the free-energy expansion by Jacobs *et al.*,[44] but by taking the Fourier transform one finds $\propto q^4P_q^4$ which is of higher order than the $\eta$ term used here.

In a seminal paper, Hornreich *et al.*[45] discussed a multicritical point of a different type, which they called a Lifshitz point. In the spherical model limit they were able to calculate critical exponents and the shape of the phase boundaries of second-order and first-order transitions in the vicinity of the Lifshitz point.[46] Let us return to the above free-energy density to give a definition[2] of the Lifshitz point. At an ordinary paraelectric to ferroelectric phase transition the coefficient $\alpha$ changes sign. If we have an additional incommensurate phase we need the $\kappa$ and $\lambda$ terms, and at the Lifshitz point $\kappa=0$. Higher-order terms in the expansion are needed for stabilization. Converting $\alpha=0$, $\kappa=0$ to variables in the extended DIFFOUR model we find $A=0$, $C=4$ (for $D=-1$). This is exactly the position of the Lifshitz point found in Sec. V. There is another analogy between Landau theory and the DIFFOUR model: Michelson[47] showed that for systems with uniaxial polarization the phase transition lines separating the paraelectric phase from the incommensurate phase and the incommensurate phase from the ferroelectric phase are tangent at the Lifshitz point. This feature is also present in Figs. 4 and 5.

Let us now discuss some properties of the solutions found in Landau theory. Ground states minimize the total free energy

$$F=\frac{1}{d}\int_0^d f(z)dz, \tag{7.4}$$

and can be found by solving the Euler-Lagrange equation

$$\lambda \frac{d^4P}{dz^4} - \kappa \frac{d^2P}{dz^2} - \eta\left[P\left(\frac{dP}{dz}\right)^2 + P^2\frac{d^2P}{dz^2}\right] + \alpha P + \beta P^3 = 0. \tag{7.5}$$

Golovko[48] was able to obtain exact solutions for some special values of the parameters in a slightly more general free-energy density [he added a term $(\gamma/6)P^6$ to the expansion (7.2)]. However, his method is not general and we will not discuss it further. Instead we follow a different approach: numerically solving[42] Eq. (7.5) shows that the solutions contain practically only one harmonic, the amplitude of higher harmonics is at most 3.5% of the former.

As usual in Landau theory only the coefficient $\alpha$ is temperature dependent: $\alpha = \alpha_0(T - T_c)$. It is found that between the high-temperature paraelectric solution

$$P(z) = 0, \quad F = 0, \tag{7.6}$$

and the low-temperature ferroelectric solution

$$P(z) = \sqrt{-\frac{\alpha}{\beta}}, \quad F = -\frac{\alpha^2}{4\beta}, \tag{7.7}$$

an incommensurate solution exists. Just below the paraelectric-incommensurate transition at $\alpha_i = \alpha_0(T_i - T_c) = \kappa^2/4\lambda$ it has the form[48]

$$P(z) = \rho_0 \cos(qz), \quad F = -\frac{(\alpha_0 - \alpha)^2}{2(3\beta + 2\eta q_0^2)}. \tag{7.8}$$

The amplitude $\rho_0$ and wave vector $q$ are given by

$$\rho_0^2 = \frac{4(\alpha_0 - \alpha)}{3\beta + 2\eta q_0^2},$$

$$q = q_0\left(1 + \frac{\eta}{8\kappa}\rho_0^2\right), \tag{7.9}$$

$$q_0^2 = -\frac{\kappa}{2\lambda}.$$

The $\eta$ term makes the incommensurate phase less stable when $\eta$ is positive, implying that the transition temperature from the incommensurate state to the ferroelectric state increases as $\eta$ increases. See also the discussion by Tolédano.[4] In the discrete model a positive $E$ term is responsible for this effect.

## VIII. CONCLUSIONS AND OUTLOOK

In this paper we have calculated various properties of an extension of the DIFFOUR model. For this purpose a next-nearest-neighbor generalization of the effective potential method was developed. The shape of the paraelectric phase boundary was proven rigorously, elaborating on a former proof which only included nearest-neighbor interactions. We found that the phase diagram changes considerably due to the extra $E$ term, but the transition at the paraelectric phase boundary does not depend on $E$. Positive $E$ favors longer-period solutions.

By taking thermal fluctuations in two different regimes into account the parameters $A$ and $C$ can be considered as effectively temperature dependent. For $C$ this holds only for nonzero $E$, which explains the relevance of this extra term. This has strong consequences for two experimentally easy accessible quantities: the temperature dependence of the modulation wave vector, and the ratio between the slopes of the soft phonon mode in the ferroelectric and paraelectric phases ($R$ parameter).

Although lattice and continuum models have some features in common, the differences are more striking. A lattice model would be a more natural choice than the phenomenological Landau treatment of incommensurate phases. Discrete models do not need *ad hoc* lock-in terms to explain different commensurate and incommensurate phases. Complex phase diagrams can in principle be obtained using a simple Hamiltonian which takes into account the discreteness of a lattice.

The $Sn_2P_2(S_{1-x}Se_x)_6$ crystal family seems to be an excellent system for our future research: it is uniaxial, has an exceptional Lifshitz point in the composition-temperature phase diagram, shows crossover effects from order-disorder to a displacive type of phase transition, and displays an interesting modulation wave vector behavior. All these phenomena can in principle be explained by the extended DIFFOUR model.

## ACKNOWLEDGMENTS

We thank Stephan Eijt for drawing our attention to this problem and Alexey Rubtsov for providing us with the results of the Monte Carlo calculations.

## APPENDIX A: EXACT RESULTS FOR PARAELECTRIC AND FERROELECTRIC PHASES

In this Appendix explicitly calculated phase boundaries are given for the extended DIFFOUR model. We first consider $E = 0$ and then discuss the effect of $E \neq 0$. Let us start with writing $V$ in the form

$$V = \sum_n \left\{\frac{a}{2}x_n^2 + \frac{1}{4}x_n^4 + c x_n x_{n-1} + d x_n x_{n-2}\right\}, \tag{A1}$$

with $d = \pm 1$. The remaining parameters $a, c, d$ are the tilde parameters defined in Eq. (2.2) after normalization of $\tilde{B}$ and $\tilde{D}$. Let us now try to write this as

$$V = \sum_n \left\{p(x_n - q x_{n-1} - r x_{n-2})^2 + \frac{1}{4}x_n^4\right\}. \tag{A2}$$

Comparison of the two expressions yields

$$p(1 + q^2 + r^2) = \frac{a}{2},$$

$$p(-2q + 2qr) = c, \tag{A3}$$

$$-2pr = d.$$

From this one can see that if it is possible to write the potential in this form and $a$ is positive, then $p$ is positive. Elimi-

nating $q$ and $r$ from the above equations yields the following fourth-order polynomial equation (assuming nonzero $a$, $c$, and $d$):

$$16p^4+(16d-8a)p^3+(8d^2+4c^2-8ad)p^2 +(4d^3-2ad^2)p+d^4=0. \tag{A4}$$

First consider the $d=+1$ case. Equation (A4) then has the following complex solutions:

$$p=\frac{1}{8}(-2+a+\sqrt{(2+a)^2-4c^2} \pm\sqrt{2}\sqrt{-4+a^2-2c^2+(-2+a)\sqrt{(2+a)^2-4c^2}}), \tag{A5}$$

$$p=\frac{1}{8}(-2+a-\sqrt{(2+a)^2-4c^2} \pm\sqrt{2}\sqrt{-4+a^2-2c^2-(-2+a)\sqrt{(2+a)^2-4c^2}}). \tag{A6}$$

The first requirement for having a real solution is that $(2+a)^2-4c^2\geqslant 0$, i.e., $a\geqslant -2+2|c|$. Consider the first two solutions (A5). First look at $|c|\geqslant 4$. Then for $a\geqslant -2+2|c|$ we find $(-2+a)\sqrt{(2+a)^2-4c^2}>0$. And for the first term in the root we find $-4+a^2-2c^2>2c^2-8|c|\geqslant 0$. So for $|c|\geqslant 4$ the only requirement for having a real (positive, $a>0$) solution is $a\geqslant -2+2|c|$. For $|c|<4$ we have $-4+a^2-2c^2+(-2+a)\sqrt{(2+a)^2-4c^2}=0$ for $a=2+\frac{1}{4}c^2$. It can be seen that the argument of the root is positive for $a>2+\frac{1}{4}c^2$. So, for $|c|<4$ the requirement for having a real (positive, $a>0$) solution is: $a\geqslant 2+\frac{1}{4}c^2$ (then $a>-2+2|c|$ automatically holds too).

The requirements for $|c|\geqslant 4$ and $|c|<4$ form a continuous line in the $a-c$-parameter space. Above this line $V$ can be written as Eq. (A2) with $p$ positive. Therefore $V\geqslant 0$. The lower bound is reached by the trivial solution which always exists, so the paraelectric phase is the ground state above this line. In Sec. IV it is shown that the above line corresponds exactly with the stability lines of the trivial solution, showing that the modulated phases arise from the destabilization of the trivial solution due to the condensation of a soft phonon mode.

In case $d=-1$ the solutions of the fourth order polynomial equation are

$$p=\frac{1}{8}(2+a+\sqrt{(-2+a)^2-4c^2} \pm\sqrt{2}\sqrt{-4+a^2-2c^2+(2+a)\sqrt{(-2+a)^2-4c^2}}), \tag{A7}$$

$$p=\frac{1}{8}(2+a-\sqrt{(-2+a)^2-4c^2} \pm\sqrt{2}\sqrt{-4+a^2-2c^2-(2+a)\sqrt{(-2+a)^2-4c^2}}). \tag{A8}$$

Look at the two solutions (A7). The first condition is $a\geqslant 2+2|c|$. $(2+a)$ is positive if this requirement is fulfilled. Further, $-4+a^2-2c^2\geqslant 2c^2+8|c|\geqslant 0$. So, here we have only one requirement for all $c$, namely, $a\geqslant 2+2|c|$. Above this line the paraelectric phase is the ground state.

With the same sort of reasoning we can also try to prove that for certain parameter values the ground state is ferroelectric. Here we work with the following form of $V$ (with $D=\pm 1$):

$$V=\sum_n \left\{\frac{A}{2}x_n^2+\frac{1}{4}x_n^4+\frac{C}{2}(x_n-x_{n-1})^2+\frac{D}{2}(x_n-x_{n-2})^2\right\}. \tag{A9}$$

We try to write this as

$$V=\sum_n \left\{\frac{A}{2}x_n^2+\frac{1}{4}x_n^4+P(x_n-Qx_{n-1}-Rx_{n-2})^2\right\}. \tag{A10}$$

Comparison of the two expressions yields

$$\begin{aligned} P(1+Q^2+R^2)&=C+D,\\ P(-2Q+2QR)&=-C,\\ -2PR&=-D. \end{aligned} \tag{A11}$$

If there exists a solution and $C+D$ is positive, then $P$ is positive. Rewriting the above equations yields the following fourth-order polynomial equation (assuming nonzero $C$ and $D$):

$$16P^4+(-32D-16C)P^3+(24D^2+16CD+4C^2)P^2 +(-8D^3-4CD^2)P+D^4=0. \tag{A12}$$

For the case $D=-1$ the complex solutions are

$$P=\frac{1}{4}(-2+C\pm\sqrt{C}\sqrt{-4+C}), \tag{A13}$$

both having multiplicity 2. For $0<C<4$ the solution is not real. For $C\geqslant 4$ the solution is real. In order to have a positive solution we must have $C+D>0$, so $C>1$. So, for $C>4$ the potential can be written as Eq. (A10) with $P$ positive. So

$$V\geqslant\sum_n \left\{\frac{A}{2}x_n^2+\frac{1}{4}x_n^4\right\}. \tag{A14}$$

The ferroelectric phase, which exists if $A<0$, reaches this lower bound. So for $B=1, D=-1, A<0$ the ground state is ferroelectric for $C>4$. In terms of the tilde parameters: for $\tilde{B}=1, \tilde{D}=1, \tilde{A}<-2-2\tilde{C}$, the ferroelectric phase is the ground state for $\tilde{C}<-4$.

For $D=+1$ the complex solutions are

$$P=\frac{1}{4}(2+C\pm\sqrt{C}\sqrt{4+C}). \tag{A15}$$

For $-4<C<0$ the solution is not real. For $C\geqslant 0$ the solution is real. In that case $P$ is positive. For $B=1$, $D=1$, $A<0$ the ferroelectric phase is the ground state for $C\geqslant 0$. In other words: for $\tilde{B}=1$, $\tilde{D}=-1$, $\tilde{A}<2-2\tilde{C}$ the ferroelectric phase is the ground state for $\tilde{C}\leqslant 0$. In terms of the tilde parameters analogous statements about the antiferroelectric phase can easily be made ($\tilde{C}\leftrightarrow-\tilde{C}$).

In case $E\neq 0$ the following holds: the parts of the phase diagram where the paraelectric phase is the ground state in the DIFFOUR model ($E=0$) also belong to the paraelectric phase for this extended model for all allowed values of $E$. In this extended model there are no other parts of the phase diagram where the trivial solution is the ground state, because the stability conditions for this solution are the same as in the DIFFOUR model (see Sec. IV).

For the ferroelectric phase the statements are less rigorous: if the ferroelectric phase is the ground state in the DIFFOUR model ($E=0$), then it is also the ground state in the extended model for $E>0$. Again we can prove that $V\geqslant\Sigma_n\{(A/2)x_n^2+(B/4)x_n^4\}$. However, for positive $E$ the part of the phase diagram where the ferroelectric phase is the ground state becomes bigger.

## APPENDIX B: EFFECTIVE POTENTIAL METHOD FOR NEXT-NEAREST NEIGHBORS

In this appendix, which is based on the account given by Griffiths,[33] we discuss how the EPM can be generalized to be applicable to systems in which there is next-nearest-neighbor interaction. Consider a classical one-dimensional chain of atoms. The total potential energy of the system is given by

$$H=\sum_{n=-\infty}^{\infty}\{V(x_n)+W(x_{n+1},x_n)+D(x_{n+2},x_n)\}. \tag{B1}$$

So, interactions up to next-nearest neighbors are included. The effective potential method that is used to find ground states for systems with interaction with first neighbors, can also be used for systems where second neighbor interaction is included. Instead of a scalar variable at site $n$, one now has to deal with a vector consisting of the values for $x$ for two adjacent atoms.[32] Writing $\mathbf{x}_n=(x_{2n},x_{2n-1})$ the above potential energy is of the form

$$H=\sum_n K(\mathbf{x}_n,\mathbf{x}_{n-1}), \tag{B2}$$

with

$$\begin{aligned}K(\mathbf{x}_n,\mathbf{x}_{n-1})=&V(x_{2n})+V(x_{2n-1})+W(x_{2n},x_{2n-1})\\&+W(x_{2n-1},x_{2n-2})+D(x_{2n},x_{2n-2})\\&+D(x_{2n-1},x_{2n-3}).\end{aligned} \tag{B3}$$

The fact that here a vector at site $n$ is considered does not change the EPM and the proofs given for this method.[28,32–34] The solution can be found by solving

$$\eta+R(\mathbf{x}_n)=\min_{\mathbf{x}_{n-1}}\{R(\mathbf{x}_{n-1})+K(\mathbf{x}_n,\mathbf{x}_{n-1})\}. \tag{B4}$$

Here $\eta$ is 2 times the ground-state energy per particle. The vector consists of two components with respect to which one has to minimize. Because of this minimization over two components, which has to be performed frequently, the numerical procedures based on discretization of the range of possible $x_n$ values will take a very long time. The method we used is slightly different. Consider the $n$th couple of adjacent atoms. Couple $(n-1)$ does not consist of two other atoms as is the case above. Instead, the right atom of couple $(n-1)$ is the same as the left atom of couple $n$. In this case only a minimization over one atomic degree of freedom (the ''position'') is left. This leads to more reasonable computation times. The fact that couple $(n-1)$ is not independent of couple $n$ requires an adaptation of the proof of the existence of a solution both in the continuous case and in the discretized case used for numerical procedures. We only give an outline of the method, proofs of the existence of solutions and generalization to systems with interactions up to $s$th neighbors are to be given in a separate paper.[35] The method for deriving the equations and the numerical procedures[34] for solving the equations remain essentially the same. Numerical calculations suggest that the error in $\eta$ has a cubic dependence on the grid size rather than the quadratic dependence for the Frenkel-Kontorova model.[32]

Let us give the following explanation[30] for the method: Imagine that a system described by Eq. (B1) is in its ground state. If we now change the positions of two adjacent atoms, the surrounding atoms will in general also change their positions in order to minimize the total energy. This net energy change caused by the deformation of one couple will be called the effective two-particle potential. This will describe the energy cost as a function of the positions of two adjacent atoms. At site $n$, the effective two-particle potential $R(x_{n+1},x_n)$, due to the presence of the atoms $i<n$, can be formally written as

$$\begin{aligned}R(x_{n+1},x_n)\equiv\min_{i<n}\Bigg\{&\sum_{i\leqslant n+1}[V(x_i)+W(x_i,x_{i-1})\\&+D(x_i,x_{i-2})-\eta]\Bigg\},\end{aligned} \tag{B5}$$

where the minimum is taken over all atomic positions $x_i$ with $i<n$ and $\eta$ is the (unknown) ground-state energy per particle. By rewriting this equation, one obtains

$$\begin{aligned}R(x_{n+1},x_n)=\min_{x_{n-1}}\min_{i<n-1}\Bigg\{&\sum_{i\leqslant n}[V(x_i)+W(x_i,x_{i-1})\\&+D(x_i,x_{i-2})-\eta]+V(x_{n+1})+W(x_{n+1},x_n)\\&+D(x_{n+1},x_{n-1})-\eta\Bigg\},\end{aligned} \tag{B6}$$

which gives

$$\eta + R(x_{n+1},x_n) = V(x_{n+1}) + W(x_{n+1},x_n) + \min_{x_{n-1}}[R(x_n,x_{n-1}) + D(x_{n+1},x_{n-1})]. \tag{B7}$$

This is the minimization eigenvalue equation for $R$. The same procedure can be followed for the effect of the atoms $i>n+1$. The effective two-particle potential due to these atoms is called $S(x_{n+1},x_n)$, which gives

$$\eta + S(x_{n+1},x_n) = V(x_n) + W(x_{n+1},x_n) + \min_{x_{n+2}}[S(x_{n+2},x_{n+1}) + D(x_{n+2},x_n)]. \tag{B8}$$

The total effective two-particle potential $F(x_{n+1},x_n)$ of a couple of adjacent atoms in a double infinite chain, is given by

$$F(x_{n+1},x_n) = R(x_{n+1},x_n) + S(x_{n+1},x_n) - V(x_{n+1}) - V(x_n) - W(x_{n+1},x_n), \tag{B9}$$

where the last three terms are subtracted on the right side to avoid double counting.

Equations (B7) and (B8) can also be obtained in another way.[32,33] Let $\tilde{R}_N(x_{n+1},x_n)$ be the minimal energy of a chain of $N$ atoms with the constraint that the atoms $N$ and $N-1$ are at fixed positions $x_{n+1}$ and $x_n$, respectively, while the other atoms are free to rearrange themselves in an optimal way so as to minimize the total energy. This leads to

$$\tilde{R}_2(x_{n+1},x_n) = V(x_{n+1}) + V(x_n) + W(x_{n+1},x_n), \tag{B10}$$

$$\tilde{R}_3(x_{n+1},x_n) = V(x_{n+1}) + V(x_n) + W(x_{n+1},x_n) + \min_{x_{n-1}}[V(x_{n-1}) + W(x_n,x_{n-1}) + D(x_{n+1},x_{n-1})] = V(x_{n+1}) + W(x_{n+1},x_n) + \min_{x_{n-1}}[\tilde{R}_2(x_n,x_{n-1}) + D(x_{n+1},x_{n-1})], \tag{B11}$$

$$\tilde{R}_{N+1}(x_{n+1},x_n) = V(x_{n+1}) + W(x_{n+1},x_n) + \min_{x_{n-1}}[\tilde{R}_N(x_n,x_{n-1}) + D(x_{n+1},x_{n-1})]. \tag{B12}$$

Now assume that for $N\to\infty$, $\tilde{R}_N(x_{n+1},x_n)$ approaches some function $R(x_{n+1},x_n)$ plus a constant proportional to $N-2$:

$$\tilde{R}_N(x_{n+1},x_n) \to R(x_{n+1},x_n) + (N-2)\,\eta. \tag{B13}$$

In that case Eq. (B7) follows. However, it is not clear that Eq. (B13) will always be satisfied. But by imposing a special boundary condition, namely

$$\tilde{R}_2(x_{n+1},x_n) = R(x_{n+1},x_n), \tag{B14}$$

Equation (B13) will be satisfied exactly.[32] The previous boundary condition is the same as saying that the left-most couple experiences the effective two-particle potential instead of the true two-particle potential. The minimum energy of this system as a function of the positions of the two right-most atoms is given by $R+N\eta$. Assuming that $R$ is a bounded function, the energy per particle of such a system will tend to $\eta$ as $N\to\infty$. $\eta$ is thus the average energy per particle in any ground state, since the extra boundary condition only changes the total energy by a term of order 1. So $R$ is the effective two-particle potential for the right-most couple of a semi-infinite chain. The same is true for $S$ for the left-most couple of a semi-infinite chain extending to the right. $F$ is the total effective two-particle potential for a couple in a double-infinite chain. $R$, $S$, and $F$ can, of course, only be defined up to an additive constant.

In the above derivations the problems arising from the summation of an infinite number of terms in Eq. (B5) are neglected. In fact, one considers local deformations of length $M$, with the limit $M\to\infty$. This will be explained below. Define the effective two-particle potential due to the local deformation of length $M$ as

$$R^{(M)}(x_{n+1},x_n) \equiv \min_{n+1-M<i<n}\left\{\sum_{n+3-M<i\leqslant n+1}[K(x_i,x_{i-1},x_{i-2}) - \eta] + [K(x_{n+3-M},x_{n+2-M},u_{n+1-M}) + K(x_{n+2-M},u_{n+1-M},u_{n-M}) - 2\eta]\right\}, \tag{B15}$$

where $u_i$ refers to the ground-state value for atom $i$, and where we have introduced

$$K(x_{n+1},x_n,x_{n-1}) \equiv V(x_{n+1}) + W(x_{n+1},x_n) + D(x_{n+1},x_{n-1}). \tag{B16}$$

The right-hand side of Eq. (B15) can be rewritten as

$$R^{(M)}(x_{n+1},x_n) = \min_{x_{n-1}}[R^{(M-1)}(x_n,x_{n-1}) + K(x_{n+1},x_n,x_{n-1}) - \eta]. \tag{B17}$$

It is reasonable to assume that in the limit $M\to\infty$: $R^{(M)}(x_{n+1},x_n)\to R^{(M-1)}(x_{n+1},x_n)$ (because $x_{n+2-M}\to u_{n+2-M}$). Writing $R(x_{n+1},x_n) = \lim_{M\to\infty} R^{(M)}(x_{n+1},x_n)$ the minimization eigenvalue equation results. In the second version of obtaining the equations it is clear that it is, in fact, the limit of local deformations, however, with the boundary condition that the left most couple of atoms experiences the effective two-particle potential. Here, one should take the length of the chain going to infinity in order to let $\eta$ go to the ground-state energy per particle. The above explanation also holds for $S$. It is best to picture the situation as a local deformation of the ground state.

Now, the nonlinear minimization eigenvalue equations for $R$ and $S$ are rewritten.[32,33] The eigenvalue equation for $R$ now becomes

$$\eta + R(x_{n+1},x_n) = \min_{x_{n-1}}[R(x_n,x_{n-1}) + K(x_{n+1},x_n,x_{n-1})]. \tag{B18}$$

Let the function $L$ be defined by

$$L(x_{n+1},x_n) = S(x_{n+1},x_n) - V(x_{n+1}) - V(x_n) - W(x_{n+1},x_n). \tag{B19}$$

The minimization eigenvalue equation for $S$ can now be rewritten as

$$\eta + L(x_{n+1},x_n) = \min_{x_{n+2}}[L(x_{n+2},x_{n+1}) + K(x_{n+2},x_{n+1},x_n)]. \tag{B20}$$

In terms of $R$ and $L$ one has

$$F(x_{n+1},x_n) = R(x_{n+1},x_n) + L(x_{n+1},x_n). \tag{B21}$$

In fact, there may be multiple solutions of the eigenvalue equation, not only differing by a trivial constant.[32,33] The existence of different solutions is related to the existence of different degenerate ground states. The general solution is given by

$$R(x_{n+1},x_n) = \min_{\alpha}[R_\alpha(x_{n+1},x_n) + K_\alpha]. \tag{B22}$$

The $R_\alpha$ correspond to the pure phases and the $K_\alpha$ are arbitrary constants.

For each solution of the minimization eigenvalue equation for $R$ [Eq. (B18)], a $\tau$ map can be defined,[32,33] where $\tau(x_{n+1},x_n) = \{(x_n,x_{n-1})\}$ with $x_{n-1}$ one of the values for which the minimum on the right-hand side of Eq. (B18) is achieved. An $R$ orbit is defined as

$$\forall n: \quad (x_n,x_{n-1}) \in \tau(x_{n+1},x_n) \Rightarrow \eta + R(x_{n+1},x_n) = R(x_n,x_{n-1}) + K(x_{n+1},x_n,x_{n-1}). \tag{B23}$$

Similarly, for the minimization eigenvalue equation for $L$ [Eq. (B20)], a $\sigma$ map can be defined, where $\sigma(x_{n+1},x_n) = \{(x_{n+2},x_{n+1})\}$ with $x_{n+2}$ one of the values for which the minimum on the right-hand side of Eq. (B20) is achieved. An $L$ orbit is defined as

$$\forall n: \quad (x_{n+2},x_{n+1}) \in \sigma(x_{n+1},x_n) \Rightarrow \eta + L(x_{n+1},x_n) = L(x_{n+2},x_{n+1}) + K(x_{n+2},x_{n+1},x_n). \tag{B24}$$

A ground state is both an $R$ orbit and an $L$ orbit. Therefore it can be proven that for a ground state

$$F(x_{n+1},x_n) = R(x_{n+1},x_n) + L(x_{n+1},x_n) = F(x_n,x_{n-1}). \tag{B25}$$

So, $F$ is constant on the positions of two adjacent atoms in a ground state, which is logical since it is the effective two-particle potential.

Numerical procedures are based on a discretized version of the system. In that case, for each ground state there is a solution for the eigenvalue equation for which there is a path from each point to the ground state in the corresponding $\tau$ graph.[34] So, the situation is as follows. There is a local deformation of length $M$ (with $M \to \infty$), in a chain coinciding with a particular ground state for $\pm\infty$. This ground state corresponds to a certain solution of the eigenvalue equation. The deformation is such that atoms $n$ and $n+1$ have values $x_n$ and $x_{n+1}$. By applying the corresponding $\tau$ map one can obtain the positions of the atoms left from $n$. For the discretized system one will finally reach the ground state in this way (in the continuous case it is supposed to converge to the ground state). The same can be done for the atoms right from $n+1$ by applying the $\sigma$ map. From this picture it is clear that the ground state is both an $R$ orbit and an $L$ orbit. In fact, the $\tau$ map and the $\sigma$ map may be multivalued. So, the atomic positions of the atoms (say) left from $n$ do not have to be unique. The deformation can have parts consisting of minimizing cycles (cycles of minimal energy) different from the ground-state configuration at $\pm\infty$. In the $\tau$ graph one can go directly to the minimizing cycle corresponding to the ground-state configuration at $-\infty$, or one can first stay for some time in another minimizing cycle if this exists. If there are several solutions for $R$ and $S$ (with several corresponding $\tau$ and $\sigma$ maps), there are several possibilities to construct $F$. It will often be logical to take the ground states, toward which the chain converges at $-\infty$ and $+\infty$, the same. The numerical algorith we used is an adapted version of the one discussed by Floria and Griffiths.[34]

Here an example will be given to show that it is important that in fact limits of finite deformations are considered. Suppose that the ground state is ferroelectric, with two degenerate ground states: $x_n = x = \pm l$ where $l \neq 0$. If the deformation is just infinite as suggested in Eq. (B5) the value of $R(l,l)$ should be the same as the value for $R(-l,-l)$. However, something else is seen. Two solutions can be found corresponding to the two ground states. In the solution corresponding to the solution $x_n = l$, $R(-l,-l)$ has a higher value than $R(l,l)$. The difference is the defect energy, the energy cost for going from the $+l$ phase to the $-l$ phase. [The defect energy (and the defect configuration) can also be calculated using the $\tau$ map.] From this it can be seen that the deformation is in fact embedded in the ground state $u_i = +l$ at $-\infty$ (in the limit $M \to \infty$: $x_{n+2-M} \to u_{n+2-M}$ where $u_{n+2-M} = +l$, or for the second version: the left most couple of atoms in the finite chain experiences the effective two-particle potential corresponding to the ground state $u_i = +l$).

It can also be expected that $F$ has local minima at the positions of two adjacent atoms in metastable states. However, since only two atoms are at a fixed position, while the other atoms are free to rearrange themselves in an optimal way, this may not be the case. When changing the positions of two adjacent atoms by an infinitesimal amount, the changes of the other atomic positions in the metastable state does not have to be infinitesimal. Therefore it is not necessarily true that there is a local minimum in $F$ for positions of two adjacent atoms in a metastable state. When there are no other atomic positions in the metastable state (a period 1 solution), $F$ does have a local minimum. When the lowest metastable state has positions of two adjacent atoms which are not seen in a ground state (which will often be the case), there will be a local minimum in $F$ for these two positions. In that case the energy cannot be lowered by changing the other atoms by any amount, since the only states which have lower

energy are ground states and these cannot be reached since the positions of the two adjacent atoms under consideration are not in a ground state (and the changes of them should be infinitesimal). By following the development of the shape of $F$ one may also investigate the kind of phase transitions that are involved. For example, a discontinuous change in the set of points where $F$ achieves its global minimum, indicates a first-order transition.[33]

*Electronic address: guidovr@sci.kun.nl
†Present address: Instituut-Lorentz for Theoretical Physics, Niels Bohrweg 2, Leiden, NL-2333 CA, The Netherlands.

[1] P. Bak, Rep. Prog. Phys. **45**, 587 (1982).
[2] W. Selke, in *Phase Transitions and Critical Phenomena*, edited by C. Domb and J. L. Lebowitz (Academic Press, London, 1992), Vol. 15, p. 1.
[3] T. Janssen and A. Janner, Adv. Phys. **36**, 519 (1987).
[4] J. C. Tolédano and P. Tolédano, *The Landau Theory of Phase Transitions* (World Scientific, Singapore, 1987), p. 215.
[5] A. D. Bruce, R. A. Cowley, and A. F. Murray, J. Phys. C **11**, 3591 (1978).
[6] I. Aramburu, G. Madariaga, and J. M. Pérez-Mato, Phys. Rev. B **49**, 802 (1994).
[7] J. Yeomans, in *Solid State Physics*, edited by H. Ehrenreich and D. Turnbull (Academic Press, San Diego, 1988), Vol. 41, p. 151.
[8] V. L. Pokrovsky and A. L. Talapov, *Theory of Incommensurate Crystals* (Harwood Academic Publishers, New York, 1984).
[9] W. Brill and K. H. Ehses, Jpn. J. Appl. Phys., Part 1 **24-2**, 826 (1985); H. G. Unruh, F. Hero, and V. Dvořák, Solid State Commun. **70**, 403 (1989).
[10] J. L. Ribeiro, M. R. Chavea, A. Almeida, J. Albers, A. Klöpperpieper, and H. E. Müser, J. Phys.: Condens. Matter **1**, 8011 (1989).
[11] W. F. Wreszinski and S. R. Salinas, *Disorder and Competition in Soluble Lattice Models* (World Scientific, Singapore, 1993).
[12] Z. Y. Chen and M. B. Walker, Phys. Rev. Lett. **65**, 1223 (1990); Phys. Rev. B **43**, 5634 (1991).
[13] Z. Y. Chen and M. B. Walker, Phys. Rev. B **43**, 760 (1991); I. Folkins, M. B. Walker, and Z. Y. Chen, *ibid.* **44**, 374 (1991).
[14] T. Janssen, Z. Phys. B: Condens. Matter **86**, 277 (1992).
[15] J. Hlinka, T. Janssen, and M. Quilichini, Ferroelectrics **155**, 257 (1994).
[16] R. Israël, R. de Gelder, J. M. M. Smits, P. T. Beurskens, S. W. H. Eijt, Th. Rasing, H. van Kempen, M. M. Maior, and S. F. Motrija, Z. Kristallogr. **213**, 34 (1998).
[17] S. W. H. Eijt, R. Currat, J. E. Lorenzo, P. Saint-Grégoire, B. Hennion, and Yu. M. Vysochanskii, Eur. Phys. J. B **5**, 169 (1998).
[18] S. W. H. Eijt, R. Currat, J. E. Lorenzo, P. Saint-Grégoire, S. Katano, T. Janssen, B. Hennion, and Yu. M. Vysochanskii, J. Phys.: Condens. Matter **10**, 4811 (1998).
[19] S. W. H. Eijt and M. M. Maior, J. Phys. Chem. Solids **60**, 631 (1999).
[20] A. V. Gommonai, A. A. Grabar, Yu. M. Vysochanskii, A. D. Belyaev, V. F. Machulin, M. I. Gurzan, and V. Yu. Slivka, Fiz. Tverd. Tela **23**, 3602 (1981) [Sov. Phys. Solid State **23**, 2093 (1981)]; Yu. M. Vysochanskii and V. Yu. Slivka, Usp. Fiz. Nauk **162**, 139 (1992) [Sov. Phys. Usp. **35**, 123 (1992)].
[21] C. C. Becerra, Y. Shapira, N. F. Oliveira, Jr., and T. S. Chang, Phys. Rev. Lett. **44**, 1692 (1980); Y. Shapira, C. C. Becerra, N. F. Oliveira, Jr., and T. S. Chang, Phys. Rev. B **24**, 2780 (1981).
[22] R. Folk and G. Moser, Phys. Rev. B **47**, 13 992 (1993); I. Nasser and R. Folk, *ibid.* **52**, 15 799 (1995); A. Abdel-Hady and R. Folk, *ibid.* **54**, 3851 (1996).
[23] J. Hlinka, T. Janssen, and V. Dvořák, J. Phys.: Condens. Matter **11**, 3209 (1999).
[24] T. Janssen, in *Incommensurate Phases in Dielectrics*, edited by R. Blinc and A. P. Levanyuk (North-Holland, Amsterdam, 1986), Vol. 1, p. 67.
[25] S. V. Dmitriev, T. Shigenari, A. A. Vasiliev, and K. Abe, Phys. Rev. B **55**, 8155 (1997).
[26] J. S. W. Lamb, J. Phys. A **25**, 355 (1992).
[27] T. Janssen and J. A. Tjon, Phys. Rev. B **25**, 3767 (1982).
[28] R. B. Griffiths and W. Chou, Phys. Rev. Lett. **56**, 1929 (1986).
[29] C. S. O. Yokoi, L. H. Tang, and W. Chou, Phys. Rev. B **37**, 2173 (1988).
[30] M. Marchand, K. Hood, and A. Caillé, Phys. Rev. B **37**, 1898 (1988).
[31] W. Chou and R. J. Duffin, Adv. Appl. Math. **8**, 486 (1987).
[32] W. Chou and R. B. Griffiths, Phys. Rev. B **34**, 6219 (1986).
[33] R. B. Griffiths, in *Fundamental Problems in Statistical Mechanics*, edited by H. van Beijeren (North-Holland, Amsterdam, 1990), Vol. VII, p. 69.
[34] L. M. Floria and R. B. Griffiths, Numer. Math. **55**, 565 (1989).
[35] K. J. H. van Bemmel (unpublished).
[36] Y. Ishibashi, J. Phys. Soc. Jpn. **60**, 212 (1991).
[37] S. Radescu, I. Etxebarria, and J. M. Pérez-Mato, J. Phys.: Condens. Matter **7**, 585 (1995).
[38] A. N. Rubtsov, J. Hlinka, and T. Janssen, Phys. Rev. E **61**, 126 (2000).
[39] A. D. Bruce, Adv. Phys. **29**, 117 (1980).
[40] S. Padlewski, A. K. Evans, C. Ayling, and V. Heine, J. Phys.: Condens. Matter **4**, 4895 (1992).
[41] P. Sollich, V. Heine, and M. T. Dove, J. Phys.: Condens. Matter **6**, 3171 (1994).
[42] Y. Ishibashi and H. Shiba, J. Phys. Soc. Jpn. **45**, 409 (1978).
[43] V. Dvořák, in *Lecture Notes in Physics. Modern Trends in the Theory of Condensed Matter*, edited by A. Pekalski and J. Przystawa (Springer, Berlin, 1980), Vol. 115, p. 447.
[44] A. E. Jacobs, C. Grein, and F. Marsiglio, Phys. Rev. B **29**, 4179 (1984); A. E. Jacobs, *ibid.* **33**, 6340 (1986).
[45] R. M. Hornreich, M. Luban, and S. Shtrikman, Phys. Rev. Lett. **35**, 1678 (1975).
[46] R. M. Hornreich, M. Luban, and S. Shtrikman, Phys. Lett. **55A**, 269 (1975); Physica A **86**, 465 (1977).
[47] A. Michelson, Phys. Rev. B **16**, 577 (1977); **16**, 585 (1977).
[48] V. A. Golovko, Zh. Eksp. Teor. Fiz. **94**, 182 (1988) [Sov. Phys. JETP **67**, 316 (1988)].